applied sciences

MDPI

Article

Multi-Step Design Optimization for the Improvement of an Outer-Rotor Brushless Direct Current Motor

Chun-Yu Hsiao * and Soe Min Htet

Department of Electrical Engineering, Tatung University, Taipei 104, Taiwan; g11102025@o365.ttu.edu.tw
* Correspondence: yu30156@gmail.com; Tel.: +886-21822928 (ext. 6364)

Abstract: Brushless Direct Current (BLDC) motors have seen significant improvements across various electrical applications. The growing focus on motor design research highlights the BLDC motor's superior efficiency compared to traditional motors, which consume more power. BLDC motors are compact, lightweight, energy-efficient, and easy to control, making them ideal for modern applications. This study aims to enhance BLDC motor design and performance by employing the Taguchi method, Response Surface Methodology (RSM), and Finite Element Method (FEM) for multi-stage optimization. A 26-watt BLDC electric fan motor is the reference model for this study. The Taguchi method helps identify optimization points, guiding further enhancements in the second stage. The study proposes a design with improved output power, torque, and efficiency. The final design achieves a 15% higher energy efficiency than the reference model, with a 10 W increase in output power and a 0.032 Nm increase in maximum torque. The FEM analysis using JMAG software v 21.2 validates the proposed design, which shows improved configurations compared to the reference model, demonstrating the efficiency of the optimization techniques for BLDC motor design.

Keywords: outer-rotor BLDC motor; Taguchi method; response surface methodology (RSM); finite element method (FEM); magnetic flux density; torque; efficiency; output power

check for updates

Citation: Hsiao, C.-Y.; Htet, S.M. Multi-Step Design Optimization for the Improvement of an Outer-Rotor Brushless Direct Current Motor. *Appl. Sci.* **2024**, *14*, 4302. https://doi.org/10.3390/app14104302

Academic Editor: Gerard Ghibaudo

Received: 13 March 2024
Revised: 2 May 2024
Accepted: 14 May 2024
Published: 19 May 2024

Copyright: © 2024 by the authors. Licensee MDPI, Basel, Switzerland. This article is an open access article distributed under the terms and conditions of the Creative Commons Attribution (CC BY) license (https://creativecommons.org/licenses/by/4.0/).

1. Introduction

BLDC motors are becoming popular for electrical applications and industrial processes and are replacing traditional induction motors. According to the International Energy Agency (IEA) analysis report, the global electricity consumption in motors accounts for more than 46% of the total electricity [1,2]. The significance of traditional motors in industrial production is that they account for the most significant power consumption. This power consumption is one of the facts of global warming and climate change. The Paris Agreement, with Intended Nationally Determined Contributions (INDCs), is aimed at contributing to carbon dioxide reduction [3], and we also supported the industrial process to replace the BLDC motor instead of using a traditional motor. The BLDC motors can be used in many electrical applications, such as electric fans, water pumping, rolling machines in various industries, and electric vehicles [4]. The performance of BLDC motors is better than that of other motors, and their electricity consumption is lower. BLDC motors can also help save energy, slow global warming, and be eco-friendly [5]. In the worldwide market of electric fans, the BLDC motor demand is increasing yearly. In 2023, a report predicted that the US dollar would go from USD 9.6 billion to USD 15.2 billion by 2025. Increasing the demand for BLDC motors is a big jump [6]. Moreover, the BLDC motor can achieve higher efficiency and lower operation noise than other motors [3].

There are several studies on optimizing the design of the BLDC motors using either Taguchi or RSM methods. In [7–10], the BLDC motor design was optimized by using the Taguchi method, whereas the studies presented in [11,12] used the RSM approach to achieve the optimal design of a motor. Most of the studies used either the Taguchi method or RSM alone. However, in [13], the author combined these two approaches to achieve a

multi-step optimization of an Interior Permanent Magnet Synchronous Motor. However, this approach has yet to be applied to optimize BLDC motors.

A novel two-step optimization algorithm for a BLDC motor design was developed to fill the research gap. The first step uses the Taguchi method to optimize seven parameters of the motor and then passes it on to the FEM analysis to obtain the preliminary optimal settings. The second step applies the RSM to refine the design, focusing on the top three critical variables that significantly impact the performance. This multi-step approach leverages the strengths of both methods: the Taguchi method, which can be used for a wide range of variables, and RSM for a small number of variables. The effectiveness of this hybrid strategy is validated by comparing the proposed model's motor design's performance using the FEM with previous results. This method efficiently combines the benefits of each optimization technique to improve motor performance. This proposed optimization approach is used to develop the optimized motor design by following the framework shown in Figure 1.

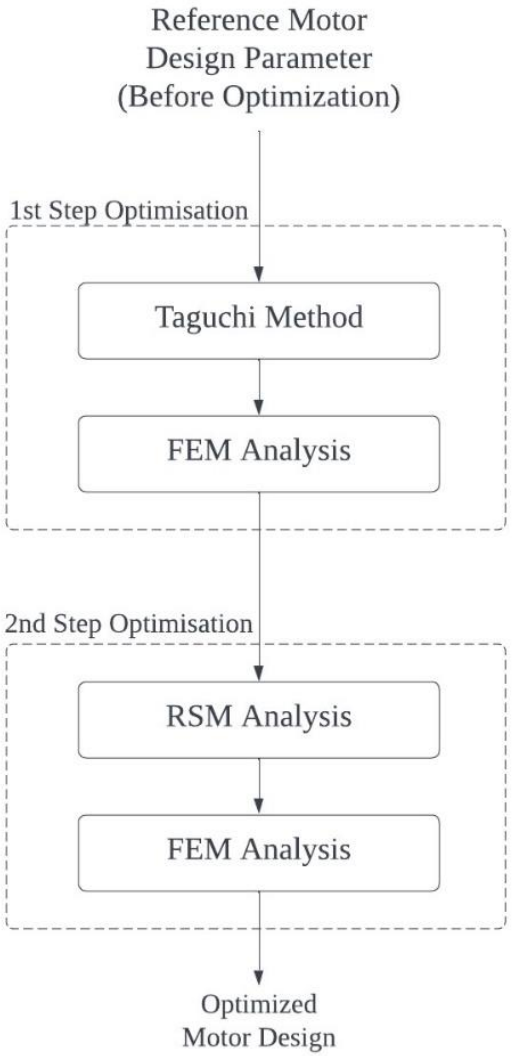

Figure 1. Flow diagram of proposed motor design.

As a preliminary study, we conducted a market survey on electric fans to select our reference motor systematically. According to the market survey, 54.7% of the participants had agreed to use the energy-saving BLDC motor electric fan, as shown in Figure 2. Based on the survey result, the BLDC motor was selected as a reference design, and the measured parameter of the reference motor was used to optimize the design using the multi-step optimization approach.

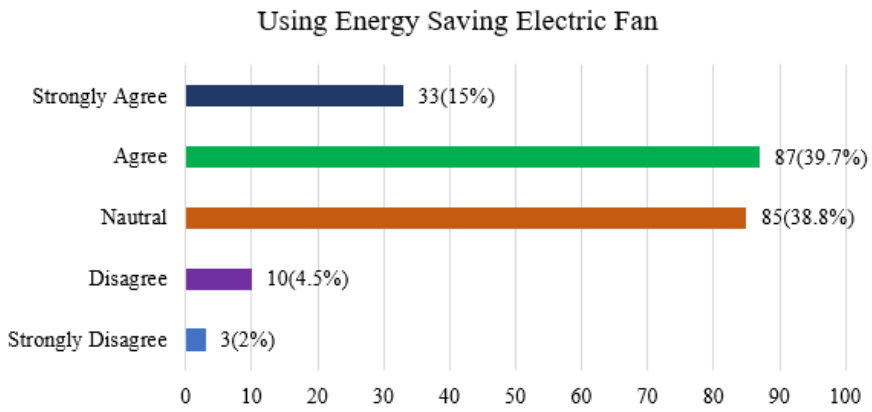

Figure 2. Result of our market survey on using energy-saving electric fan.

2. Configuration of Reference Model's Design and Materials

The design calculation of the outer-rotor BLDC motor can be used in the following equation. This motor can be calculated using the torque development equation; T_{max} is the torque development of the motor in Nm, P is the number of poles, B_g is the air gap flux density in the electrical degree of 120 in Wb/m^2, I_c is the current through a conductor in amperes, n_s is the number of stator slots, L is the conductor length in mm, and R_{inner} is the inner radius of the stator in mm [14]:

$$T_{max} = 2\ P\ B_g\ I_c\ n_s\ L\ R_{inner} \quad (1)$$

$$B_g = \varnothing_{magnet}\ A_g \quad (2)$$

$$\varnothing_{magnet} = \frac{\varnothing_r}{1 + k\frac{R_g}{R_m}} \quad (3)$$

The magnetic flux density is shown in Equation (3). The magnetic flux density is the relation between the resistance of the air gap and the magnet. The coefficient of reactance ***k*** is a constant value of the magnetic material [15].

A higher efficiency percentage means that the motor is more efficient, with less power lost to inefficiencies, while a lower percentage indicates higher losses and less efficient energy conversion. The efficiency of a motor is expressed in percentages. P^{out} is the output power of the motor and the mechanical power generated by the motor in Watts (W), typically measured at the shaft. P_{loss} is the total power lost within the motor due to various inefficiencies like the electrical resistance in W, friction, windage, iron losses, and other factors contributing to energy loss. The P_{in} is the total electrical power consumed by the motor from its power source in W [14,15]. We can calculate the efficiency as follows:

$$\eta = \frac{P_{out} - P_{loss}}{P_{in}} \quad (4)$$

Equations (5) and (6) show the relative permittivity of the material in terms of the electric displacement vector {D} in (C/m^2); [e] is the Piezoelectric stress constant matrix (C/m^2), $[e^S]$ is the permittivity matrix (F/m), {S} is the Strain vector, and {E} is the vector for the electric field intensity (N/C) [16].

$$\{D\} = [e]\{S\} - [e^S]\{E\} \quad (5)$$

$$\left[e^S\right] = \begin{bmatrix} E_{11} & E_{12} & E_{13} \\ E_{21} & E_{22} & E_{23} \\ E_{31} & E_{32} & E_{33} \end{bmatrix} \quad (6)$$

The material of China steel 50CS1300 [17,18] can be used in the reference motor model of the stator and rotor parts. According to the information provided by the JMAG, the specifications for the configuration of the China steel material are shown in Figure 3. This material has a magnetic flux range of 1.5 T to 1.8 T. In the reference motor, the magnetic flux does not exceed the 1.8 T value. In this study, we used this material in the proposed motor design.

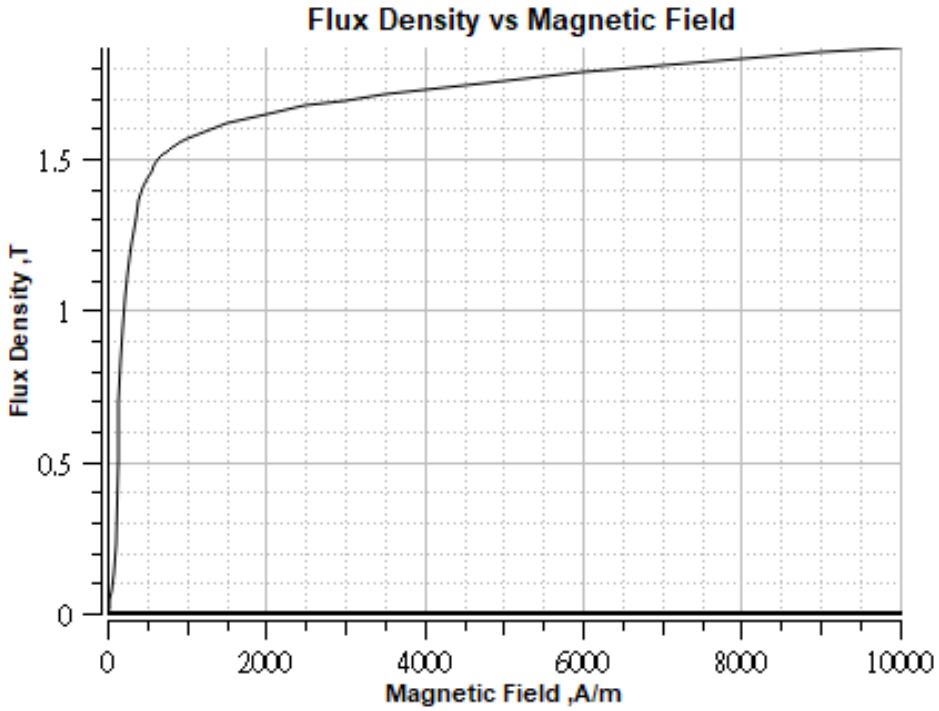

Figure 3. The relationship between the flux density and magnetic field for the stator and rotor material in the reference model [17].

The magnet is magnetized to the saturation point in a closed circuit, and the B-H curve characteristics of the Ferrite magnet and the NMF-6C magnet are used in the rotor part in the reference motor design. Figure 4 provides a hysteresis loop of the relationship between the magnetic induction (B) and the magnetizing force (H). This curve describes the magnetic field strength of the negative coercivity value of −270 kA/m, which is an approach to the zero value of the magnetic flux density based on the information provided by JMAG. In this case, the coercivity of the magnetic field strength reduces the magnetization to zero after the magnet has been saturated [17,18].

The parameter of this reference motor was measured, and the measured parameter results are shown in Tables 1 and 2.

Table 1. Specification of reference electric fan motor parameters.

Parameter	Value	Unit
Outer diameter	55	mm
Inner diameter	45	mm
Stator bore diameter	20	mm
Gap length	0.3	mm
Number of slots	12	
Number of poles	10	
Rated voltage	24	V
Rated current	3	A
Speed	5500	rpm
Connection type	Y	

Table 2. Input parameter values of reference motor design.

Parameter	Value	Unit
Depth of stator slot (D_{ss})	10	mm
Width of stator tooth (W_{st})	4.5	mm
Width of stator slot opening (W_{so})	2	mm
Height of stator tooth tang (H_{st})	0.801	mm
Angle of stator tooth tang (α)	27	degree
Number of turns (N)	82	
Magnet thickness (M_t)	3.5	mm
Stack height (H)	4.5	mm

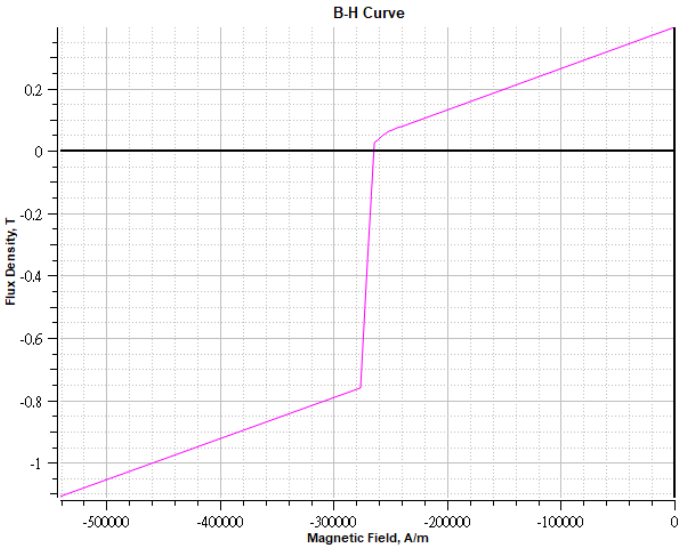

Figure 4. The relationship between the B-H curves of the reference model's rotor material [17].

In this experiment, we used JMAG software, which is a commonly used software in this field, and several publications are based on the simulation of this software [9,14,17]. The reference motor's design and the modeling of the motor using JMAG software use the specifications and data presented in Tables 1 and 2. This table includes dimensions, material properties, and specific electromagnetic characteristics that are relevant to the reference motor design. These parameters involve setting up the motor geometry model and defining the suitable material, as shown in Figure 5, of the rotor and the stator of the reference motor design using the JMAG software.

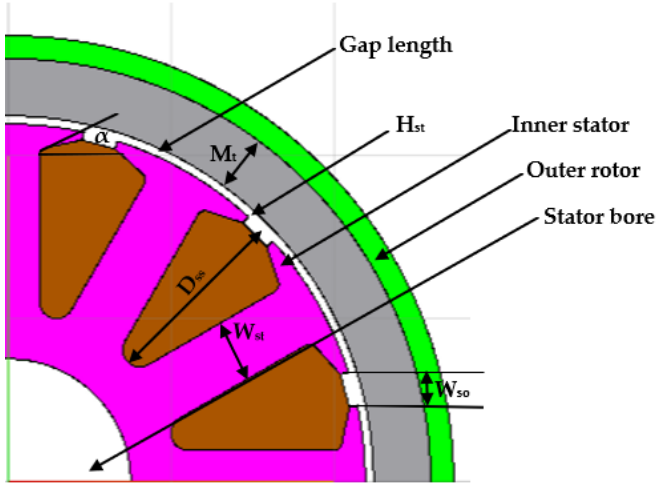

Figure 5. Cross-section of reference motor.

In this study, the motor design is measured in the actual simulation of a motor-testing machine from the motor-testing company [18]. The motor-testing machine data and software simulation results are the same. The testing machine's result for the reference motor can be seen in Figure 6. This figure shows the reference design of the motor in terms of efficiency, output power, and voltage. These output values are used to improve the studied design for optimization.

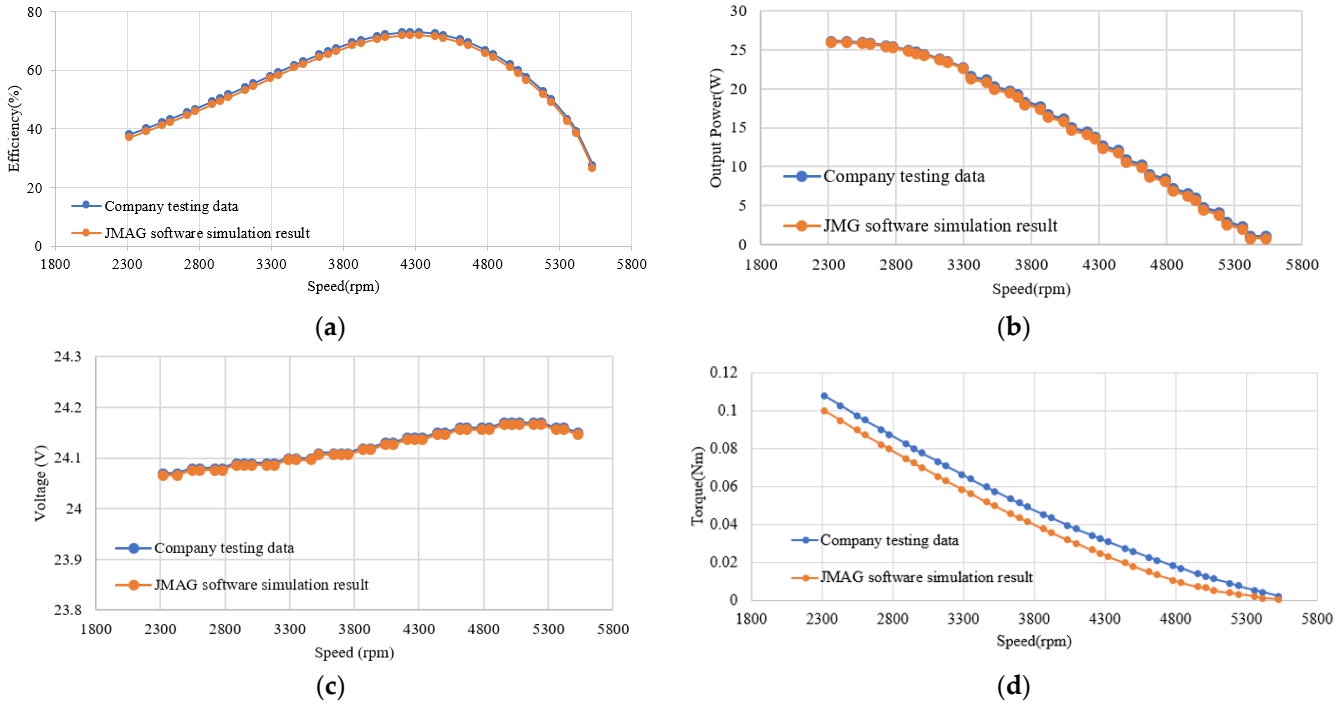

Figure 6. Comparison between the company's testing data and JMAG software results: (**a**) efficiency, (**b**) output power, (**c**) voltage, and (**d**) torque.

The comparison of testing data and JMAG software simulation results is shown in Figure 6. According to the results in Figure 6, the maximum value of the motor's output power, voltage, and efficiency are shown in Table 3.

Table 3. Comparison of the maximum result of each parameter between the testing machine and software.

Parameter	Testing Machine [18]	Software
Efficiency	72.92%	72.76%
Voltage	24.09 V	24.06 V
Output power	26.14 W	26.06 W
Torque	0.1076 Nm	0.100 Nm
Speed	5528 rpm	5528 rpm

This similarity between the simulation and test data is a critical factor in the study, as it confirms the reliability and accuracy of the simulation software used in this study. These results show that the software simulation of the reference motor is similar to the actual data from the testing machine. Therefore, the software-simulated motor can be used as the reference motor for optimization.

In addition, this study also carried out an in-depth application of the Taguchi method and RSM. These methodologies are core components of this research and are designed to increase efficiency and effectiveness within our field. The research process is optimized through these technologies, and our target successfully improves overall efficiency.

3. Taguchi Method and Response Surface Methodology (RSM)

This section will be divided into three parts: the Taguchi method, RSM, and the Taguchi method based on RSM (multi-step). A detailed explanation of each approach will be described in the following sub-sections.

3.1. Taguchi Method

The Taguchi method is a prominent experimental design technique that can enhance a product's quality by optimizing the design parameters [19]. Table 4 shows the variance in the control factors. The factors obtained for the Taguchi method to optimize the design parameters of the control factor are selected for the reference motor part of the dimension parameters. Each control factor has different levels, representing the different settings or values that it can take. The selection of the control factor of the Taguchi method is the first consideration in the process to improve the performance of the motor design. The Taguchi method uses these specially designed matrices to study a large number of variables with a minimal number of experiments. This approach significantly reduces the time and resources needed for experimentation.

Table 4. Design variance of the control factors.

Constant	Control Factors	Orthogonal Array Levels		
		1	2	3
A	Stack height	3.5 mm	4.5 mm	5.5 mm
B	Width of stator tooth	2.8 mm	3.8 mm	4.8 mm
C	Depth of stator slot	8 mm	10 mm	12 mm
D	Width of stator slot opening	1.5 mm	2.25 mm	3 mm
E	Angle of stator tooth tang	17 deg	27 deg	37 deg
F	Number of turns	72	82	92
G	Magnet thickness	3.5 mm	4.5 mm	5.5 mm

The main objective is to improve the performance of the product or process, like a BLDC motor, by optimizing the control factors. This involves finding the best combination of the control factors' levels, which produces the most robust and high-quality outcome. By focusing on the control factors and seeking a design that is less sensitive to noise factors, the Taguchi method helps us achieve an economically efficient design. It reduces the need for expensive alterations to handle noise factors, as the optimized design inherently copes better with these variations.

In the Taguchi method, noise factors are variables that cannot be controlled or are too costly to maintain. These might include environmental conditions or usage variations in a BLDC motor. In contrast, control factors are those that can easily be adjusted. The goal is to minimize the impact of noise factors to optimize control factors [7–10,13,19,20].

In our experiment, the selected control factors for the proposed model's stack height, a value range of 3 mm to 4 mm, have been chosen. This range is determined by the motor's operating speed and its performance characteristics. At a stack height of 3 mm, the motor's speed reaches 8700 rpm. This range provides a suitable configuration for balancing the proposed model's characteristics, ensuring optimal motor performance. The control levels of the number of turns, width of slot opening, depth of stator slot, and angle of the stator tooth tang also correspond to the increased and decreased range of the torque, efficiency, and magnetic flux, which will happen within the range, as described in Table 4.

Using the Taguchi method, Table 5 shows the FEM analysis of the simulation result. This result can be the rated speed in the range of 5400 rpm, and we cannot use the exceeded value within a range. The S/N ratios of the efficiency, torque, and output power are shown in Figure 7.

Table 5. FEM analysis of Taguchi method of orthogonal array (L = 3^7).

A	B	C	D	E	F	G	η (%)	P_{out} (W)	τ_{max} (Nm)
3.5	2.8	8	1.50	17	72	3.5	65.50	26.37	0.0682
3.5	2.8	8	1.50	27	82	4.5	68.27	24.53	0.0991
3.5	2.8	8	1.50	37	92	5.5	70.24	20.95	0.1358
3.5	3.8	10	2.25	17	72	3.5	73.86	27.05	0.0692
3.5	3.8	10	2.25	27	82	4.5	77.08	27.78	0.1000
3.5	3.8	10	2.25	37	92	5.5	78.76	29.14	0.1354
3.5	4.8	12	3.00	17	72	3.5	79.25	36.21	0.0460
3.5	4.8	12	3.00	27	82	4.5	81.47	33.26	0.0706
3.5	4.8	12	3.00	37	92	5.5	82.24	32.27	0.0970
4.5	2.8	10	3.00	17	82	5.5	79.43	30.85	0.0980
4.5	2.8	10	3.00	27	92	3.5	78.87	35.03	0.0653
4.5	2.8	10	3.00	37	72	4.5	79.69	33.11	0.0753
4.5	3.8	12	1.50	17	82	5.5	82.18	28.66	0.1083
4.5	3.8	12	1.50	27	92	3.5	81.87	34.27	0.1022
4.5	3.8	12	1.50	37	72	4.5	81.74	34.07	0.0735
4.5	4.8	8	2.25	17	82	5.5	71.31	26.85	0.1038
4.5	4.8	8	2.25	27	92	3.5	71.51	32.11	0.0999
4.5	4.8	8	2.25	37	72	4.5	70.71	31.99	0.0717
5.5	2.8	12	2.25	17	92	4.5	81.05	29.08	0.0947
5.5	2.8	12	2.25	27	72	5.5	81.11	30.59	0.0668
5.5	2.8	12	2.25	37	82	3.5	80.76	33.84	0.0667

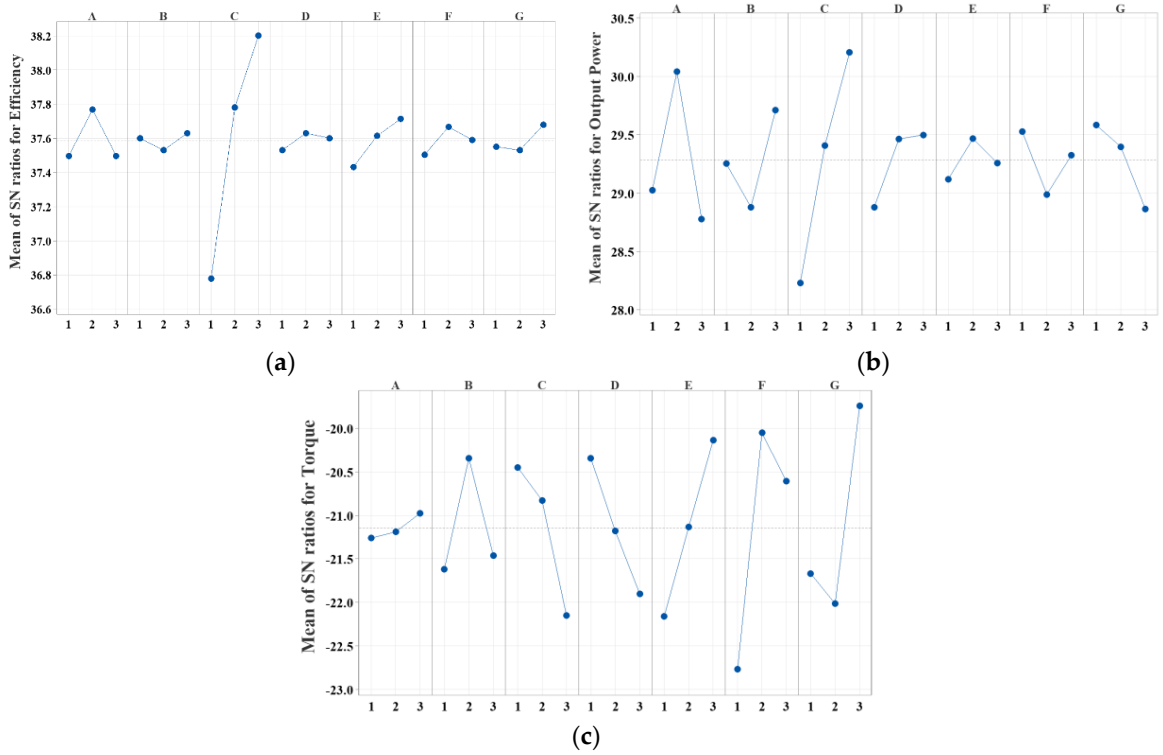

Figure 7. S/N ratios of mean to control factor for proposed model design: (**a**) S/N ratios for maximum efficiency; (**b**) S/N ratios for maximum output power; and (**c**) S/N ratios for maximum torque.

The outer-rotor BLDC motor involves various control factors: magnet thickness, stator tooth tang angle, stator slot depth, stator slot opening width, stack height, and number

of turns. This method improves the motor's performance, focusing on maximum torque, efficiency, and power. Figure 7a shows the high efficiency of the proposed model value of "level 2" for the stack height, width of stator slot opening, and number of turns. The "level 3" for the width of the stator tooth, depth of stator slot, angle of stator tooth tang, and thickness of magnet can provide the high efficiency of the reference model design. The maximum output power can achieve "level 1" for the number of turns and magnet thickness; "level 2" for the stack height and angle of the stator tooth tang; and "level 3" for the width of the stator tooth, depth of the stator slot, and width of the stator slot opening, as shown in Figure 7b. The "level 1" for the depth of the stator slot and width of the stator slot opening, the "level 2" for the width of the stator tooth and the number of turns, and the "level 3" for the angle of the stator tooth tang and magnet thickness can cause the maximum torque, as shown in Figure 7c.

Using FEM analysis for one-step optimization, Table 6 displays the difference between the proposed model using the Taguchi method and the reference model. From Table 6, we can obtain the three different design specifications for the maximum efficiency, torque, and output power. Then, to optimize further, the second-step optimization is executed to achieve higher efficiency for the motor design.

Table 6. Comparison of results for control factors for reference and proposed model using Taguchi method.

Performance		A	B	C	D	E	F	G	Results
Efficiency	Reference	2	2	1	2	3	2	2	72.76%
	Proposed	2	3	3	2	3	2	3	81.93%
	Improvement (+12.6%)								9.17%
Output Power (W)	Reference	2	2	1	2	3	2	2	26.06 W
	Proposed	2	3	3	3	2	1	1	34 W
	Improvement (+30.5%)								10 W
Torque (Nm)	Reference	2	2	1	2	3	2	2	0.098 Nm
	Proposed	3	2	1	1	3	2	3	0.130 Nm
	Improvement (+32.6%)								0.032 Nm

3.2. Respond Surface Methodology (RSM)

Respond Surface Methodology (RSM) starts with a carefully planned series of experiments. The RSM offers advantages when optimizing problems with fewer than three design variables. It helps to determine optimal values by creating a model based on statistical data, allowing for an easy exploration of the interaction effects between variables [21]. These experiments are designed to systematically vary critical factors to understand how changes in these factors affect the outcomes or responses. The design often includes central composite design (CCD), Box–Behnken design (BBD), or factorial design as the selected design, and the workflow of the RSM is shown in Figure 8 [11,12,22].

Among the options, we chose the CCD method, because it is often better for BLDC motor optimization due to its flexibility, ability to capture complex relationships (including quadratic effects), and efficient exploration of the response surface. It strikes a good balance between thoroughness and experimental count, making it suitable for scenarios where multiple factors and their interactions are critical [22].

After careful analysis of the FEM analysis outcomes and evaluation of the sample test for the optimized model derived via the Taguchi method, an enhanced design iteration was conducted employing RSM. This approach is particularly efficacious for optimizing fewer than three design variables and enables the determination of optimal responses for the objective function while accounting for interactive effects [13]. To effectively meet the performance objectives, a two-stage optimization design utilizing RSM was implemented, which capitalizes on the principal factors identified during the initial optimization phase, thus obviating the need for a comprehensive re-optimization of the entire array of motor variables. As depicted in Table 7, the design variables and their corresponding ranges for the RSM are outlined.

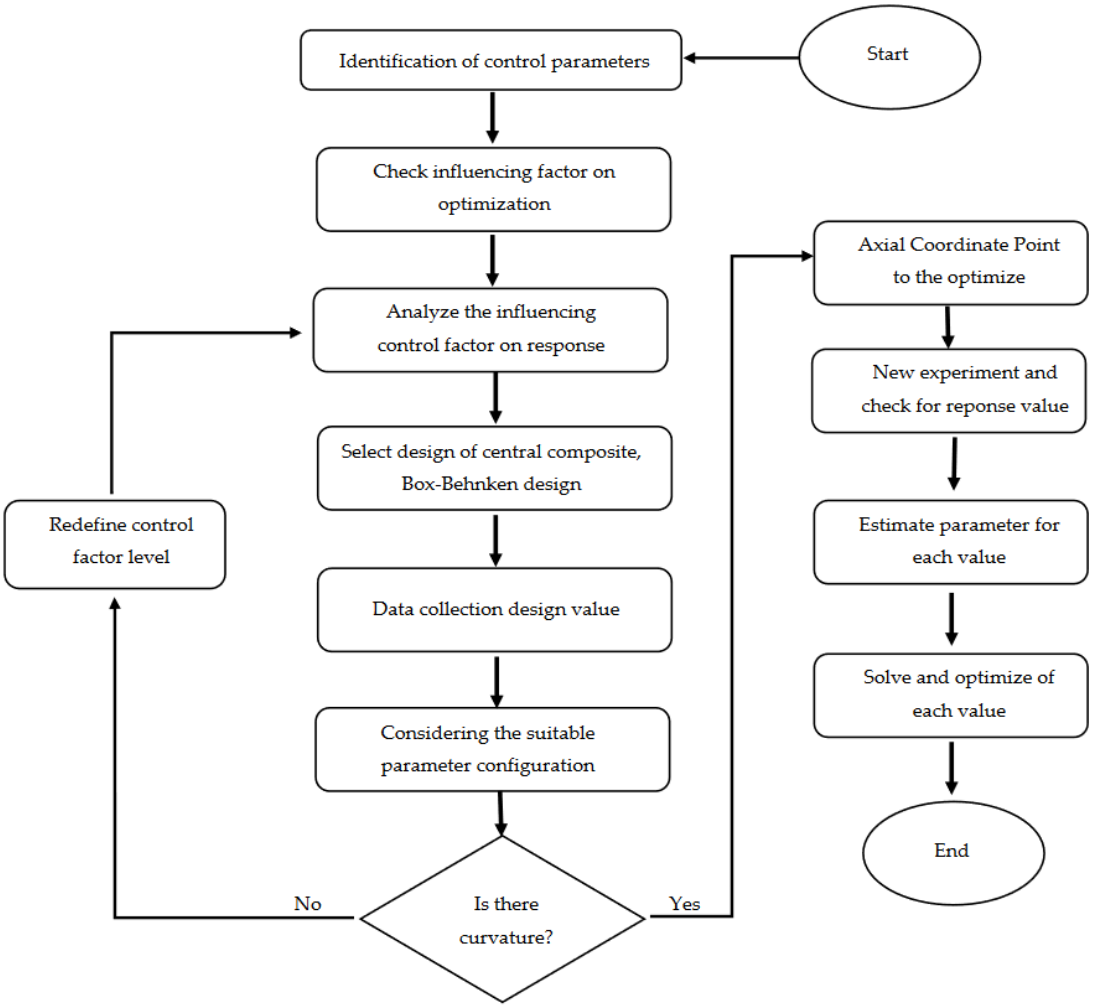

Figure 8. Organization of RSM procedure.

Table 7. FEM analysis of CCD of RSM.

Exp No	Thickness of Magnet (mm)	Width of Stator Slot Opening (mm)	Number of Turns	η (%)	P_{out} (W)	τ_{max} (Nm)
1	3.0	3.0	72	80.55	29.2824	0.0975
2	3.5	2.3	82	81.34	26.5498	0.1041
3	4.0	1.5	92	82.33	22.1713	0.0944
4	2.7	2.3	82	81.94	28.6889	0.1127
5	4.0	3.0	92	83.73	25.9793	0.0927
6	3.5	2.3	82	82.20	29.9981	0.1041
7	3.5	2.3	82	82.20	29.9981	0.1041
8	4.3	2.3	82	79.62	28.3713	0.0654
9	3.0	1.5	92	83.01	27.2877	0.1284
10	3.0	1.5	72	81.70	30.0426	0.1001
11	3.5	2.3	82	82.92	30.2034	0.1041
12	3.5	2.3	82	82.92	30.2034	0.1041
13	3.5	2.3	66	77.27	29.2334	0.0835
14	4.0	3.0	72	78.49	29.0056	0.0724
15	3.5	2.3	99	83.63	26.4092	0.1257
16	4.0	1.5	72	83.28	30.0000	0.0739
17	3.5	1.0	82	82.52	28.3235	0.1051
18	3.5	2.3	82	82.92	30.2034	0.1041
19	3.5	3.0	92	83.12	28.5026	0.1245
20	3.5	3.5	82	83.48	31.2632	0.1011

A critical parameter, the magnet thickness, was singled out from the array of variables recognized in the Taguchi optimization stage due to its significant impact on motor performance. In addition to this, two other variables, namely, the number of turns and the width of the stator slot's opening, were incorporated to further scrutinize the operational scope and efficiency of the motor. Variables that would lead to an escalation in material costs and weight were deliberately excluded from this phase. Consequently, the design variables were confined to three key factors, with their ranges being meticulously defined to ensure the structural feasibility of the BLDC motor's configuration.

When adjusting the number of turns and width of the stator slot opening, the coil diameter is modified to achieve a slot fill factor that is suitable for production. The objective function is formulated to ensure a motor efficiency of 82% or higher at a torque of 0.1 Nm or greater. Minimizing power losses leads to increased efficiency and output power, and hence, the inclusion of the output power in the objective function. The efficiency, torque, and maximum operating speed of all the design models generated by the RSM are assessed using FEM results, as presented in Table 7. Figure 9 illustrates a graph depicting the RSM optimizer, which determines the optimal values of design variables to meet the specified objective functions using Minitab v 22.0.

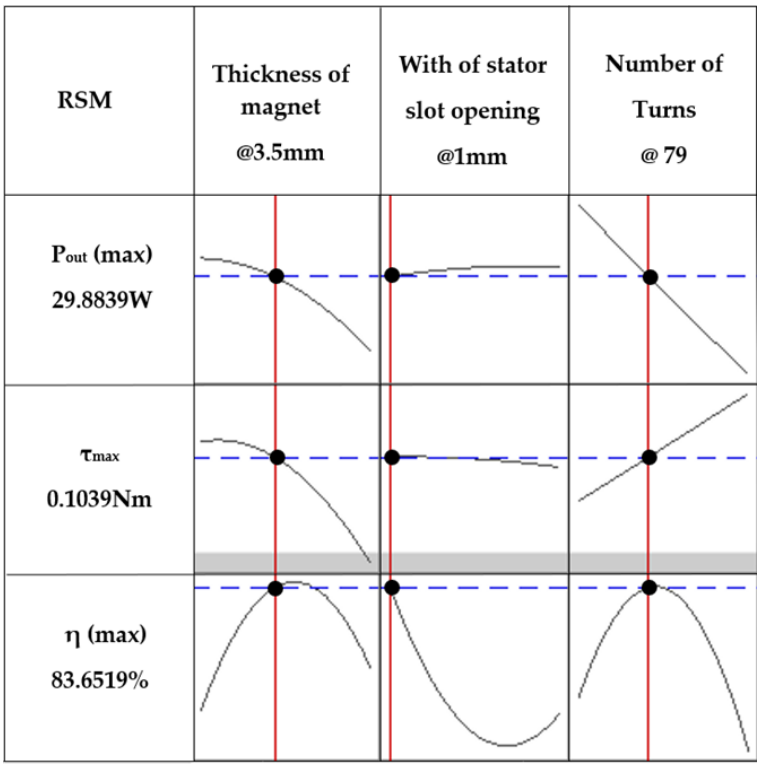

Figure 9. RSM analysis of proposed model optimization.

The motor's efficiency is affected by the thickness of the magnet, the width of the stator slot opening, and the number of turns; the output power and torque of the target level can be achieved at the maximum efficiency point, as shown in Figure 9. The thickness of the magnet is 3.5 mm, the width of the stator slot opening is 1 mm, and the number of turns is 79, which can cause maximum efficiency of 83.6519%, torque of 0.1039 Nm, and output power of 29.8839 W. Based on the results and reviewing the RSM, as shown in Figure 9, we can find the optimal design parameter value satisfying the design target.

The final result from the simulations is shown in Table 8 and demonstrates that the reference motor, compared with the Taguchi method and Taguchi method-based RSM, is under investigation using FEM analysis. The proposed (optimized) multi-step optimization can be more efficient than the Taguchi method optimization and reference motor design.

Table 8. The reference model was compared with the Taguchi method and the Taguchi-based RSM.

Performance	Reference	Proposed (Optimized)	
		Taguchi Method	Taguchi-Based RSM
Efficiency (%)	72.76	81.93	83.65
Output Power (W)	26.06	31.46	30
Torque (Nm)	0.098	0.1020	0.1039

4. Discussion

The discussion regarding the development and optimization design of an outer-rotor Brushless DC (BLDC) motor using a combination of the Taguchi method and Response Surface Methodology (RSM) for Finite Element Method (FEM) analysis involves several intricate steps and considerations. The design process begins with the basic configuration of an outer-rotor BLDC motor [10–16]. This includes determining the motor's physical dimensions, magnet type, winding patterns, and other structural elements. The outer-rotor design is specific, as the rotor is on the outside, encircling the stator. This configuration can offer benefits in specific applications compared to inner-rotor designs. Based on the FEM analysis, further adjustments might be made to the motor design to refine its performance [21–27]. This process can be repeated several times, refining the design each time based on the Taguchi method, RSM, and FEM analysis results.

The Taguchi method is employed to identify the key factors that significantly affect the motor's performance. This involves selecting control factors (like magnet thickness, number of turns, and stator part) and noise factors (factors that are not easily controlled but impact the performance). An orthogonal array is chosen, and experiments are designed to systematically vary the control factors while keeping the noise factors at bay to the extent that it is possible. Experiments based on the Taguchi design are carried out. In the case of the motor design, these could be virtual experiments using FEM analysis to simulate the motor's performance under different conditions. Under various experimental conditions, data are collected on motor performance parameters like torque, efficiency, and power output.

5. Conclusions

The conclusion to this study on BLDC motors emphasizes the significant improvements achieved in these motors for various electrical applications. There has been a consistent annual increase in research and development focused on BLDC motor design. Most researchers in motor design have identified the superior efficiency of BLDC motors compared to traditional motors. BLDC motors are noted for consuming less electrical power than conventional motors. Their design is characterized by compactness, a small size, ease of control, being energy-saving, and being lightweight. The conclusion underscores the necessity of further analyzing and improving the design of the BLDC motor to enhance its performance characteristics. The research utilized the Taguchi Method and RSM in conjunction with FEM analysis for optimizing the motor's design. The Taguchi Method initially identified the optimization points of design parameters using a reference model of an actual 26-watt BLDC electric fan motor. RSM was then employed for two-step optimization in the FEM analysis—the investigation aimed to improve structural performances in output power, torque, and efficiency. After the first step of optimization, the efficiency was 12% higher than that of the reference design, and this was further improved by 3% in the second step of optimization. Therefore, the final proposed model achieved an energy efficiency that was 15% higher than the reference design. The output power of the proposed model was also 10 Watts higher than the reference design. The study found a reduction in losses and an increase in the maximum torque by 0.032 Nm in the proposed design. The design simulation results were produced and studied using JMAG software for FEM analysis. The evaluation compared the reference model's design with the proposed design using three different methods of motor design optimization. This comparison showed that the proposed design exhibits improvements in terms of the performance of the motor design.

Author Contributions: Conceptualization, C.-Y.H.; methodology, C.-Y.H. and S.M.H.; software S.M.H.; validation, C.-Y.H. and S.M.H.; formal analysis, C.-Y.H. and S.M.H.; investigation, C.-Y.H. and S.M.H.; resources, C.-Y.H. and S.M.H.; data curation,S.M.H.; writing—original draft preparation, C.-Y.H. and S.M.H.; writing—review and editing, C.-Y.H. and S.M.H.; visualization, C.-Y.H.; supervision, C.-Y.H.; project administration, C.-Y.H. and S.M.H. All authors have read and agreed to the published version of the manuscript.

Funding: This research was fully funded by the NSTC 111-2221-E-036-010-MY2 project for the National Science and Technology Council (NSTC) in R.O.C (Taiwan), and Tatung University.

Institutional Review Board Statement: Not applicable.

Informed Consent Statement: Not applicable.

Data Availability Statement: This article contains real data results from the reference motor supported by Lutron Industrial Co., Ltd., as well as another part of the data generated to support the findings of the present study.

Acknowledgments: The authors gratefully acknowledge full funding support from the NSTC 111-2221-E-036-010-MY2 project for the National Science and Technology Council (NSTC) in R.O.C (Taiwan), Professional Equipment Support from Energy Administration, Ministry of Economic Affairs, R.O.C (Taiwan) and Taiwan Green Productivity Foundation and Tatung University. The authors would like to acknowledge the technological support from Jotactic Automotive Consulting Co., Ltd. and the Editor-in-Chief, Editor, and Reviewers for their valuable reviews.

Conflicts of Interest: The authors declare no conflicts of interest.

References

1. Căta, A.; Țăranu, B.-O.; Ienașcu, I.M.C.; Sfirloaga, P. New PVP–Ag or Pd-Doped Perovskite Oxide Hybrid Structures for Water Splitting Electrocatalysis. *Appl. Sci.* **2024**, *14*, 1186. [CrossRef]
2. Eason, G.; Noble, B.; Sneddon, I.N. On certain integrals of Lipschitzankel type involving products of Bessel functions. *Phil. Trans. Roy. Soc. Lond.* **1955**, *A247*, 529–551.
3. Shao, J. An improved microcontroller-based sensor less brushless DC (BLDC) motor drive for automotive applications. *IEEE Trans. Ind. Appl.* **2006**, *42*, 1216–1221. [CrossRef]
4. Mohanraj, D.; Aruldavid, R.; Verma, R.; Sathiyasekar, K.; Barnawi, A.B.; Chokkalingam, B.; Mihet-Popa, L. A Review of BLDC Motor: State of Art, Advanced Control Techniques, and Applications. *IEEE Access* **2022**, *10*, 54833–54869. [CrossRef]
5. Hasanbeigi, A. Utilities and Governments are Wasting Millions of Dollars Subsidizing A Wrong Technology for Motor Systems Efficiency. 2018. Available online: https://www.eeip.org/articles/detailed/b54ae3494-e0cfd5837f5693810b4fbe5/utilitiesand-governments-are-wasting-millions-of-dollars-subsidizing-awrong-technology-for-motor-s/ (accessed on 13 May 2024).
6. Ali Hasanbeigi, P.D. Infographic: The Profile of Energy Use in Industrial Motor Systems. 2017. Available online: https://www.globalefficiencyintel.com/newblog/2017/infogra-phicenergy-industrial-motor-systems (accessed on 13 May 2024).
7. Zhu, W.; Yang, X.; Lan, Z. Structure Optimization Design of High-Speed BLDC Motor Using Taguchi Method. In Proceedings of the 2010 International Conference on Electrical and Control Engineering, Wuhan, China, 25–27 June 2010; pp. 4247–4249. [CrossRef]
8. Apatya, Y.B.A.; Subiantoro, A.; Yusivar, F. Design and prototyping of 3-phase BLDC motor. In Proceedings of the 2017 15th International Conference on Quality in Research (QiR): International Symposium on Electrical and Computer Engineering, Nusa Dua, Bali, Indonesia, 22–27 July 2017; pp. 209–214. [CrossRef]
9. Hsiao, C.-Y.; Htet, S.M.; Lin, G.H.; Yang, T.H. Investigation of Design Performance in Outer Rotor BLDC Motor for Taguchi Method. In Proceedings of the 2023 IEEE 6th Student Conference on Electric Machines and Systems (SCEMS), Huzhou, China, 7–9 December 2023; pp. 1–6. [CrossRef]
10. Hsiao, H.-C.; Hsiao, C.-Y.; Huang, Y.-H.; Chien, Y.-K.; Zheng, Y.-W. Design and Economical Evaluation of Small-Capacity Motor Used in Household Appliances by Taguchi Method. In Proceedings of the 2018 IEEE Student Conference on Electric Machines and Systems, Huzhou, China, 14–16 December 2018; pp. 1–6. [CrossRef]
11. Lee, B.-H.; Hong, J.-P.; Lee, J.-H. Optimum design criteria for maximum torque and efficiency of a line-start permanent-magnet motor using response surface methodology and finite element method. *IEEE Trans. Magn.* **2012**, *48*, 863–866. [CrossRef]
12. Zhang, Y.; Xu, J.; Han, Z.; Wu, Z.; Huang, C.; Li, M. System-Level Optimization Design of Tubular Permanent-Magnet Linear Synchronous Motor for Electromagnetic Emission. In Proceedings of the 2021 13th International Symposium on Linear Drives for Industry Applications (LDIA), Wuhan, China, 1–3 July 2021; pp. 1–4. [CrossRef]
13. Cho, S.-K.; Jung, K.-H.; Choi, J.-Y. Design Optimization of Interior Permanent Magnet Synchronous Motor for Electric Compressors of Air-Conditioning Systems Mounted on EVs and HEVs. *IEEE Trans. Magn.* **2018**, *54*, 8204705. [CrossRef]

14. Hsiao, C.-Y.; Htet, S.M.; Lin, G.H.; Yang, T.H.; Lu, M.-S. Analysis on the Effect of Number of Poles and Thickness of Permanent Magnet in PMBLDC Motor. In Proceedings of the 2023 9th International Conference on Applied System Innovation (ICASI), Chiba, Japan, 21–25 April 2023; pp. 121–123. [CrossRef]
15. Zhilichev, Y. Analysis of Permanent Magnet Demagnetization Accounting for Minor B–HB–H Curves. *IEEE Trans. Magn.* **2008**, *44*, 4285–4288. [CrossRef]
16. Huner, E. Optimization of axial flux permanent magnet generator by Taguchi experimental method. *Bull. Pol. Acad. Sci. Tech. Sci.* **2020**, *68*, 409–419. [CrossRef]
17. Corporation, JSOL. JMAG, 22.0. Available online: https://www.jmag-international.com/express/ (accessed on 13 May 2024).
18. Lutron, I.; Lutron Industrial Co., Ltd. Lutron Ind. Available online: https://lutron-ind.weebly.com/ (accessed on 1 January 2024).
19. Si, J.; Zhao, S.; Feng, H.; Cao, R.; Hu, Y. Multi-objective optimization of surface-mounted and interior permanent magnet synchronous motor based on Taguchi method and response surface method. *Chin. J. Electr. Eng.* **2018**, *4*, 67–73. [CrossRef]
20. Ajamloo, A.M.; Ghaheri, A.; Afjei, E. Multi-objective Optimization of an Outer Rotor BLDC Motor Based on Taguchi Method for Propulsion Applications. In Proceedings of the 2019 10th International Power Electronics, Drive Systems and Technologies Conference (PEDSTC), Shiraz, Iran, 12–14 February 2019; pp. 34–39. [CrossRef]
21. Beeravelli, V.N.; Chanamala, R.; Rayavarapu, U.M.R.; Kancherla, P.R. An Artificial Neural Network and Taguchi Integrated approach to the optimization of performance and emissions of direct injection diesel engine. *Eur. J. Sustain. Dev. Res.* **2018**, *2*, 16. [CrossRef] [PubMed]
22. Taghinezhad, E.; Kaveh, M.; Szumny, A.; Figiel, A. Quantifying of the Best Model for Prediction of Greenhouse Gas Emission, Quality, and Thermal Property Values during Drying Using RSM (Case Study: Carrot). *Appl. Sci.* **2023**, *13*, 8904. [CrossRef]
23. Sun, Q.; Cheng, Y.; Chen, Z. Minimization of Torque Fluctuation in Disc Type In-Wheel Motor Based on Response Surface Method and FEA. In Proceedings of the 2019 IEEE 3rd International Conference on Green Energy and Applications (ICGEA), Taiyuan, China, 16–18 March 2019; pp. 85–88. [CrossRef]
24. Singh, V. Application of Artificial Neural Networks for predicting generated wind power. *Int. J. Adv. Comput. Sci. Appl. (IJACSA)* **2016**, *7*, 250–253. [CrossRef]
25. Braik, M.S. Chameleon Swarm Algorithm: A bio-inspired optimizer for solving engineering design problems. *Expert Syst. Appl.* **2021**, *174*, 114685. [CrossRef]
26. Inayathullaah, M.A.; Sivakumar, N.; Balasundaram, A.; Arul, R.; Angalaeswari, S. Time Domain Investigation of Hybrid Intelligent Controllers Fed Five-Phase PMBLDC Motor Drive. *Appl. Sci.* **2023**, *13*, 3281. [CrossRef]
27. Carev, V.; Roháč, J.; Tkachenko, S.; Alloyarov, K. The Electronic Switch of Windings of a Standard BLDC Motor. *Appl. Sci.* **2022**, *12*, 11096. [CrossRef]

Disclaimer/Publisher's Note: The statements, opinions and data contained in all publications are solely those of the individual author(s) and contributor(s) and not of MDPI and/or the editor(s). MDPI and/or the editor(s) disclaim responsibility for any injury to people or property resulting from any ideas, methods, instructions or products referred to in the content.